Defence Science Journal, Vol. 66, No. 2, March 2016, pp. 93-99, DOI : 10.14429/dsj.66.9291

Design, Testing, and Realisation of a Medium Size Aerostat Envelope

A. Kumar[*,!], S.C. Sati[*], and A.K. Ghosh[#]

[*]*Aerial Delivery Research and Development Establishment, Agra – 282 001, India*
Department of Aerospace Engineering, Indian Institute of Technology, Kanpur - 208 016, India
[!]*E-mail: ajit_kumar@adrde.drdo.in*

ABSTRACT

The design, testing and realisation aspects during the development of a medium size aerostat envelope have been presented in this paper. The payload capacity of this aerostat is 300 kg at 1 km above mean sea level. The aerostat envelope is the aerodynamically shaped fabric enclosure part of the aerostat which generally uses helium for lifting useful payloads to a specified height. The envelope volume estimation technique is discussed which provides the basis for sizing. The design, material selection, testing and realisation aspects of this aerostat envelope are also discussed. The empirical formulas and finite element analysis are used to estimate the aerodynamic, structural and other design related parameters of the aerostat. Equilibrium studies are then explained for balancing forces and moments in static conditions. The tether profile estimation technique is discussed to estimate blow by distance and tether length. A comparison of estimated and measured performance parameters during trials has also been discussed.

Keywords: Aerostat envelope, shape optimisation, payload capacity, tether profile

NOMENCLATURE

A	Reference area, $V^{2/3}$, m^2
a_v	Lift curve slope, per radian
B, B_f	Buoyancy force in kgf & N
C_D	Drag coefficient
C_{D_0}	Zero lift drag coefficient
C_L	Lift coefficient
C_{m_0}	Pitching moment coefficient about aerodynamic centre
D	Envelope maximum diameter, m
D_A	Aerodynamic drag on envelope, N
D_{H_n}, D_{w_n}	Cable element drag in horizontal & vertical direction, N
F	Total aerodynamic force acting on 1m section of envelope, N/m
F_L	Free lift in terms of fraction of gross lift
F_{ax}, F_{az}	Aerodynamic force along X- and Z-direction, N
g	Acceleration due to gravity, m/s^2
H	Operating height of aerostat, km
K	Coefficient in drag polar equation
K_t	Tether length factor
L_A	Aerodynamic lift on envelope, N
L_a	Buoyancy per unit volume, N/m^3
M, m_t	Envelope mass, kg and tether mass per unit length, kg/m
M_a	Moment about aerodynamic centre, N-m
N_b	Stress resultant due to buoyancy, N/m
p	Maximum local surface pressure, Pa
P_{eq}, P_i	Envelope pressure at equator & bottom, Pa
P_{L_a}	Payload capacity at altitude, kg
q	Dynamic air pressure, N/m^2
R, S	Radius of earth and line of sight, km
t	Envelope fabric thickness, m
T_0, T_a	Absolute temperature for ISA at sea level and at operating height, K
T_c, T_n	Tether tension at confluence point and for lower element, N
T_X, T_Z	Tether tension component in X- & Z-direction, N
U	Steady wind speed, m/s
V, V_g	Envelope volume and LTA gas volume in envelope, m^3
W, w_n	Envelope and cable element weight, N
$X_C, \bar{X}_C$	X-Distance, m and non dimensional distance from nose to confluence point
$X_G, \bar{X}_G$	X-Distance, m and non dimensional distance from nose to CG
$X_N, \bar{X}_N$	X-Distance, m and non dimensional distance from nose to aerodynamic centre
$Z_C, \bar{Z}_C$	Z-Distance, m and non dimensional distance from nose to confluence point
α	Trim angle of attack, rad
ΔT	Temperature difference between operating condition and ISA, K
ρ_a, ρ_g	Air and gas density at height, kg/m^3
ρ_{a_0}, ρ_{g_0}	Air density at ISA sea level and LTA gas density for 0 °C & ISA sea level, kg/m^3
σ	Envelope stress, Pa
θ_C, θ_n	Angle with horizontal at confluence point and for lower elements, rad

1. INTRODUCTION

An aerostat is a lighter than air object that can stay stationary in the air and is tethered to the ground. Aerostat envelope derives the lifting force mainly by the buoyant effect that results from displacement of the higher density air surrounding it. The envelope gas is generally helium because it is inert and provides adequate lifting capability. Ground based sensors have limited line of sight range due to the limitations posed

Received 28 September 2015, revised 29 January 2016, online published March 2016

by earth's curvature (horizon effect). Mounting these sensors on elevated platforms like towers, aircrafts & balloons can increase the line of sight range. The limitation of the height up to which a tower can be built, is obvious. Aircrafts have limited endurance (on-station time) of few hours whereas aerostats can remain operational continuously for days. Aerostats have been proven platforms for these sensors especially in surveillance and communication role for a variety of civil and military applications.

Aerostat systems provide help in raising the electronic payloads for increasing their line of sight range so as to overcome the terrain obstructions like trees, buildings, mountains and similar obstructions. Aerostat system is a mission-oriented vehicle with attributes like payload platform availability at high altitudes, increased line of sight coverage for payload and long on-station time. Payloads along with operational conditions are the deciding factors for the size estimation of the aerostat envelope.

Aerial Delivery Research and Development Establishment (ADRDE), Agra has developed a medium size aerostat for a gross payload capacity of 300 kg up to a height of 1 km above mean sea level with 5 days endurance. The present work explains the development aspects of this aerostat envelope. The design, material selection, testing and realisation aspects are discussed. The empirical formulas and finite element analysis are used to estimate the aerodynamic, structural and other design related parameters of the aerostat envelope. Static equilibrium analysis has also been carried out. The technique for estimating tether profile has also been discussed. A comparison study has also been carried out for the estimated performance parameters with the measured values during the limited flight trials.

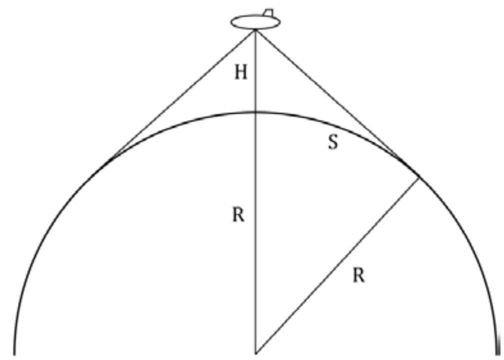

Figure 1. Geometry for line of sight coverage.

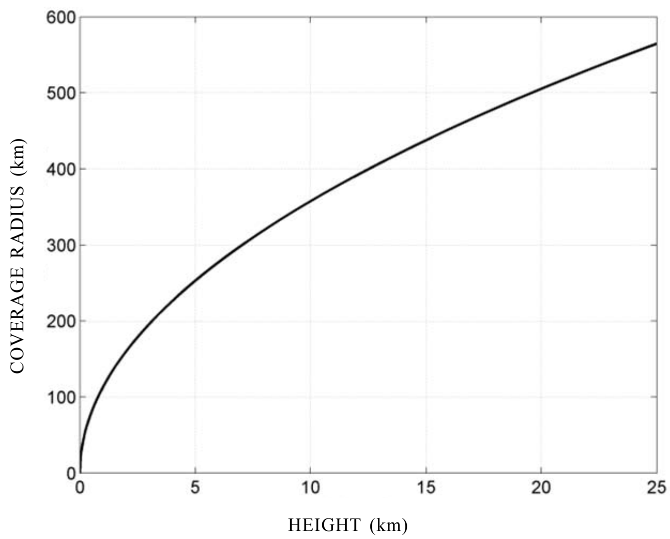

Figure 2. Coverage radius with altitude.

2. LINE OF SIGHT

The coverage area of the aerostat is determined by calculating the radial distance to the horizon from the aerostat launch point. This radial line of sight range (S) is calculated based on the height of the aerostat (H) and the Earth's radius (R) as shown in Fig. 1. Using simple geometric relation in Fig. 1, the expression for S is written as below[1]:

$$S = R\cos^{-1}\left(\frac{R}{R+H}\right) \tag{1}$$

The line of sight for a range of altitudes is plotted in Fig. 2. For a height of 1 km, the line of sight radius is about 113 km whereas for a height of 5 km, the line of sight radius is about 253 km.

3. SHAPE AND VOLUME ESTIMATION

Aerodynamically shaped envelope is required to carry payload to an altitude. The envelope should be shaped such as to have minimum drag and required lifting capability. The shape optimisation requires a comparative study of shapes in terms of the required parameters such as buoyancy capability, surface area, lift, drag, stability, stresses, blow by and ease of fabrication. The use of advanced computational tools such as computational fluid dynamics (CFD) and finite element method (FEM) may be required for this purpose[2]. Based on the requirements outlined, a particular shape has been found suitable for the present application. The shape is having elliptical front section, circular mid-section and parabolic tail section. Helium filled fins are added to the aerostat envelope for stability.

An aerostat envelope consists of main helium compartment (hull), air compartment (ballonet), fins, cordages and patches. Ballonet is an air-inflated compartment inside the hull. This is required to maintain constant differential pressure of envelope. As the envelope goes up, outside pressure decreases. Hence to maintain constant differential pressure, air is required to be pumped out from the ballonet. Similarly, when the envelope comes down, air is required to be pumped into the ballonet. Also, gases expand and contract depending on temperature rise or fall and ballonet air also caters for it. Some amount of air is also kept as reserve. Differential pressure sensor senses the pressure and electronic unit gives command to the blower or deflation valve to put air in or out from the ballonet compartment. Thus constant differential pressure is maintained.

The basis of volume estimation of an aerostat envelope is Archimedes' principle. The starting point for the volume estimation is given payload capacity and height of operation. The sequence of procedure followed for volume estimation of aerostat is presented in Fig. 3. For estimating gross lift of aerostat envelope, air density, helium density, and helium volume is required and may be written as[3, 4]:

$$B = V_g\left(\rho_a - \rho_g\right) \qquad (2)$$

$$\rho_a = \rho_{a_0}\left(\frac{T_0 - 0.0065H}{T_0}\right)^{4.254}\left(\frac{T_a}{T_a + \Delta T}\right) \qquad (3)$$

$$\rho_g = \rho_{g_0}\left(\frac{273.15}{T_a}\right)\left[\frac{\rho_a\left(T_a + \Delta T\right)}{\rho_{a_0} T_0}\right] \qquad (4)$$

The gas volume is obtained by subtracting ballonet air volume from the total envelope volume. Now the payload capacity of the aerostat envelope can be written as:

$$P_{L_a} = \left(1 - F_L\right)B - M - K_t m_t H \qquad (5)$$

The additional factors which may be required to be considered while applying the above equation include relative humidity and helium purity. The weight of aerostat envelope includes hull fabric, fin fabric, ballonet fabric, joints, adhesive, patches, cordages and accessories. For a payload capacity of 300 kg and a height of operation 1000 m AMSL, the hull volume comes out to be about 2000 m^3 with a maximum diameter of 11.1 m and fineness ratio of 3. Hull with three helium filled fins in inverted-Y configuration is selected to provide adequate stability. Figure 4 provides the payload performance of this aerostat envelope for different heights and operating conditions.

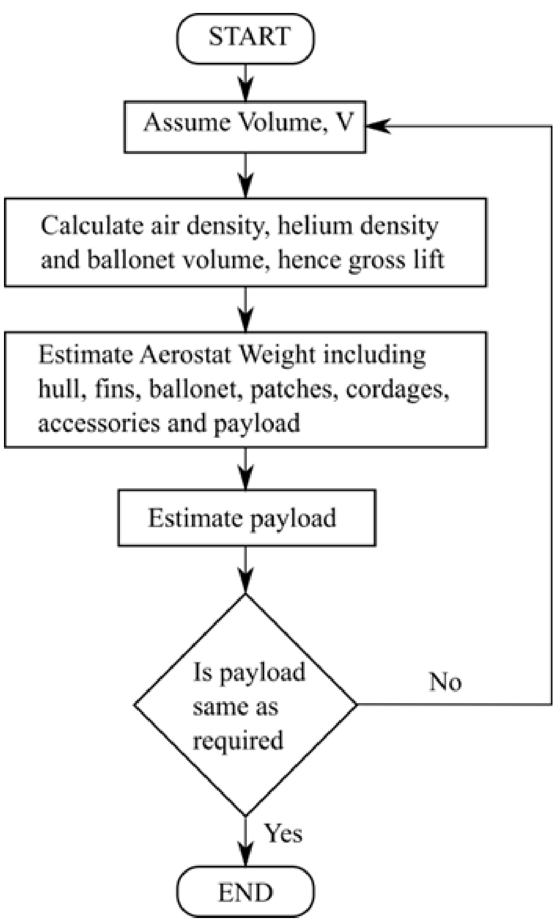

Figure 3. Flow chart for volume estimation of aerostat envelope.

4. MATERIAL SELECTION

Aerostat envelopes are made up of textile materials with hull, ballonet and fins made from coated/laminated nylon/polyester fabrics, cordages made from nylon/polyester/ Kevlar/ Vectran. The fabric used in fabrication should be selected such that it should withstand the stresses generated because of shape of the envelope or environmental conditions, which the aerostat has to sustain during its flight duration. The ideal envelope material for an aerostat should have the following properties[3]:

- High strength to weight ratio
- Resistance to environmental degradation
- High tear resistance
- Low permeability
- Joining technique that produce strong and reliable joint
- Low creep

The material for the present medium size aerostat envelope is selected as PU coated nylon fabric. Nylon provides the strength and PU coating provides an effective protection against UV rays. The cordages of aerostat envelope are made of nylon/polyester/Kevlar for high strength to weight ratio.

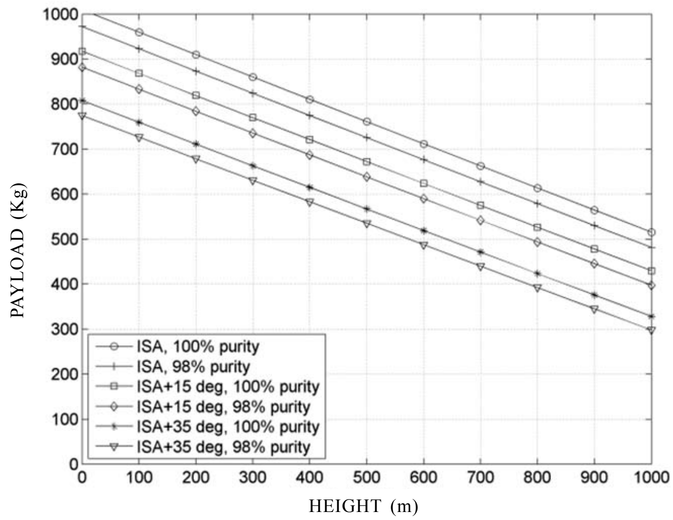

Figure 4. Payload performance of medium size aerostat envelope.

5. STRESS ANALYSIS

Stress estimation is carried out to select the envelope material of appropriate strength. Initially analytical approximation for maximum stress has been done. Envelope internal pressure (5±1 mbar) is selected, about 15 per cent more than the maximum dynamic pressure so that the nose of the envelope will not cut or dimple[5]. Using the approach as outlined[5], the maximum analytical stress is estimated as follows.

5.1 Stress due to Internal Pressure

The envelope internal pressure is assumed to be at the bottom so it is required to calculate the pressure at the envelope equator which is at a height of $D/2$ from the bottom as shown in Fig. 5. The internal pressure at envelope equator and maximum stress may be written as:

$$P_{eq} = P_i + (\rho_a - \rho_g) g \frac{D}{2} \tag{6}$$

$$\sigma_i = \frac{P_{eq} D}{2t} \tag{7}$$

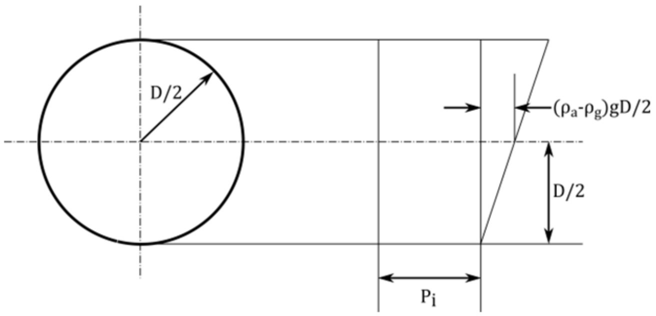

Figure 5. Internal pressure distribution on maximum diameter of aerostat envelope.

5.2 Stress due to Buoyant Lift

The maximum stress resultant due to buoyant load at altitude acting on 1m section of the envelope (Fig. 6) and the stress may be written as:

$$N_b = \frac{1}{2}\left[L_a\,(1m - section)\right] \tag{8}$$

$$\sigma_b = \frac{1}{2t}\left[(\rho_a - \rho_g) g \frac{\pi D^2}{4}\right] \tag{9}$$

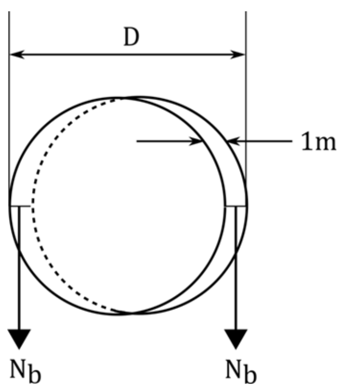

Figure 6. Buoyancy load on 1m section of aerostat envelope.

5.3 Stress due to Hull Bending Moment

The stress due to aerodynamic bending moment for design dynamic pressure at altitude for the typical hull/ suspension arrangement is:

$$\sigma_{bm} = 0.123 \frac{1}{2} \rho_a U^2 V^{1/3} \tag{10}$$

5.4 Stress due to Aerodynamic Loads

From the wind tunnel tests, the maximum local pressure was determined to be approximately $p = 0.1q\alpha$. This occurs at approx. 30 per cent aft of the leading edge. However, for this analysis it was assumed to act at maximum diameter. Therefore, the total aerodynamic force acting on 1 m section (Fig. 7) and

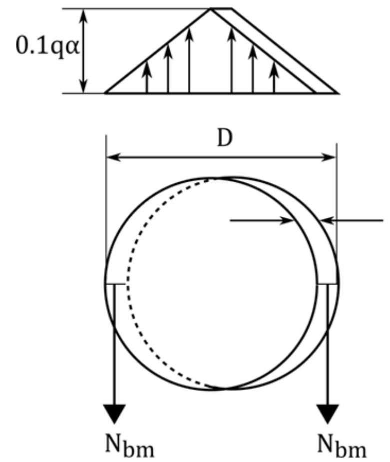

Figure 7. Load distribution on envelope due to aerodynamic bending.

the resulting stress is:

$$F = p\frac{D}{2} = 0.1q\alpha\frac{D}{2} \tag{11}$$

$$\sigma_a = \frac{1}{2t}F = 0.05q\alpha\frac{D}{2t} \tag{12}$$

The design stress on the envelope is the sum of the stresses caused by the internal pressure, buoyant lift, bending and aerodynamic loads i.e. summation of stresses in Eqns. (7), (9), (10) and (12) with a factor of safety 4 to account for uncertainties and fabric degradation[6]. Figure 8 shows the variation of maximum stress with operating aerostat parameters i.e. internal pressure, wind speed and angle of attack as well as important load cases. It is observed in Fig. 8 that for low wind speed, the dominant stress is due to internal pressure whereas for high wind speed the stresses due to aerodynamic loads and hull bending become significant. The important load cases for flying and mooring conditions are also indicated in Fig. 8 corresponding to operating wind speed.

Finite lement modelling and geometric nonlinear analysis has also been carried out for critical operational cases to estimate the distribution of stress on the aerostat envelope as well as forces in guy wires and confluence lines and tether tension[7] using the approach described[8]. Envelope has been modeled using membrane elements and lines have been modeled using rod elements. The geometry of the vehicle is symmetric about *X-Z* plane and the load cases considered in the analysis are also symmetric about this plane. Hence only right half of the aerostat is modelled and appropriate symmetric boundary conditions are applied. Along with the symmetry boundary conditions, the nodes on either side of the bracing lines of the vertical are connected by enforcing same displacements in *X* and *Z* directions to simulate the bracing symmetry behavior. The confluence point is held in all the three translational degrees of freedom. Apart from these conditions, the translation in *Z*-direction at a suitable node on the hull is also suppressed to prevent rigid body rotation (pitching).

Figure 9 shows a typical hoop stress distribution on envelope surface corresponding to load case L4 described in Fig. 8. This result indicates that maximum stress is in good agreement with analytical value and is also confined near the maximum diameter portion.

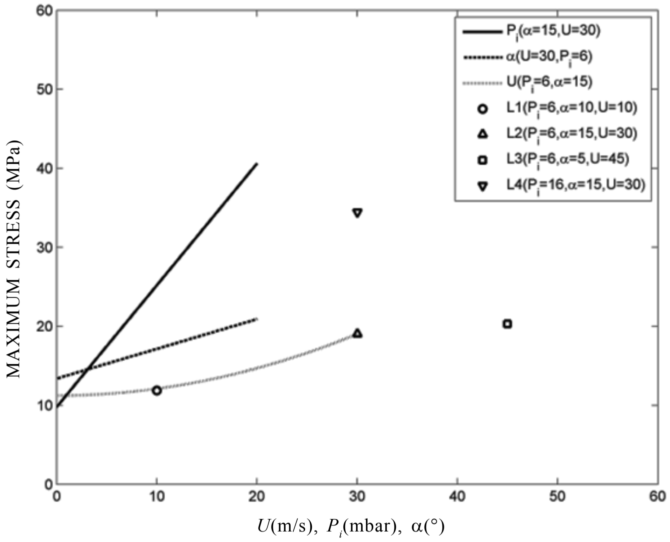

Figure 8. Variation of maximum stress on envelope.

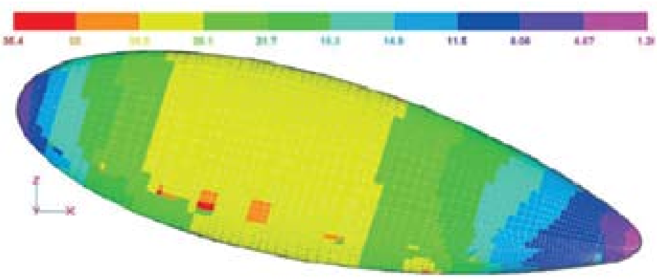

Figure 9. Finite element analysis result for the hoop stress (MPa) distribution on envelope surface.

6. EQUILIBRIUM ANALYSIS AND TETHER TENSION

The tethered aerostat configuration establishes its equilibrium under given wind conditions with a certain value of pitch angle (angle of attack or trim angle) and a blow by due to combined action of wind and tether. The blow by is the horizontal distance of aerostat from launch or anchor point. It is required to carry out equilibrium analysis to estimate this angle of attack for the entire range of wind speed. The approach presented[9] is used for this purpose. The following forces act upon the aerostat in this condition (Fig. 10).

- Gravity force (weight)
- Buoyancy force
- Tension in the tether
- Aerodynamic force

Under the action of these forces, force equilibrium along X and Z directions and moment equilibrium about the confluence point C give:

$$F_{ax} - B_f \sin\alpha + W\sin\alpha + T_X\cos\alpha - T_Z\sin\alpha = 0 \tag{13}$$

$$F_{az} + B_f \cos\alpha - W\cos\alpha + T_X\sin\alpha - T_Z\cos\alpha = 0 \tag{14}$$

$$M_a - F_{az}(X_N - X_G + X_C) + (F_{ax} - B_f\sin\alpha + W\sin\alpha) Z_C - B_f\cos\alpha(X_B - X_G + X_C) + W\cos\alpha X_C = 0 \tag{15}$$

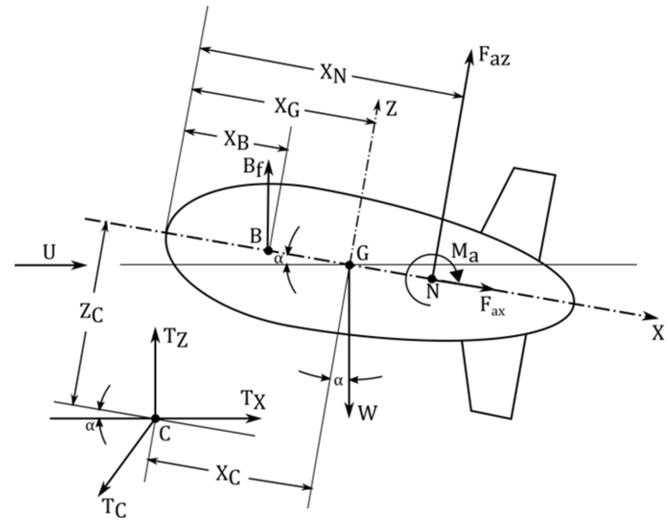

Figure 10. Force diagram for the aerostat envelope.

The aerodynamic forces F_{ax} and F_{ax} in Eqns. (13) and (14) may be written in terms of the lift and drag of the aerostat envelope[5]. We also use $C_L = a_v \sin\alpha$ and $C_D = C_{D_0} + K\alpha^2$. Eliminating T_X and T_z from Eqns. (13) and (14) and using Eqn. (15), we have

$$\frac{1}{2}\rho_a U^2 A = \frac{B_f\left\{\cos\alpha\left(\bar{X}_B - \bar{X}_G + \bar{X}_C\right) + \sin\alpha \bar{Z}_C\right\} - W\left\{\cos\alpha \bar{X}_C + \sin\alpha \bar{Z}_C\right\}}{\left[C_{m_0} - \left\{a_v\sin\alpha\cos\alpha + \left(C_{D_0} + K\alpha^2\right)\sin\alpha\right\}\left(\bar{X}_N - \bar{X}_G + \bar{X}_C\right) + \left\{a_v\sin^2\alpha + \left(C_{D_0} + K\alpha^2\right)\cos\alpha\right\}\bar{Z}_C\right]} \tag{16}$$

Equation (16) is non-linear in α. Here the distances are non-dimensionalised with respect to envelope length. The above equation is solved numerically[10] for equilibrium trim angle of attack α. The calculated value of angle of attack should lie within the specified range of $\pm$ 15 deg. Also, the tether tension and angle with horizontal for the aerostat may be written as (Fig. 10).

$$T_C = \sqrt{D_A^{\,2} + \left(B_f + L_A - W\right)^2} \tag{17}$$

$$\theta_C = \tan^{-1}\left(\frac{B_f + L_A - W}{D_A}\right) \tag{18}$$

The payload capacity, trim angle and tether tension are estimated using Eqns. (5), (16), and (17), respectively. Table 1 presents these estimated parameters considering all possible variations in aerodynamic parameters, temperature, helium purity and wind speed thereby covering the entire possible range of operating conditions. Table 1 also presents the measured values of these parameters during the limited flight trials of this aerostat. It is observed in Table 1 that both estimated and measured trim angle lie within the specified range of $\pm$ 15 degrees. Also the measured values of payload capacity, trim angle and tether tension during the limited flight trials of the aerostat lies within the estimated values for entire operating conditions.

Table 1. Comparison of estimated and actual performance of aerostat envelope

Parameter	Estimated values for entire operating conditions and wind speed 0-30 m/s	Measured values during limited trials and wind speed 0-10 m/s
Payload capacity	Min 300 kg	300 kg
Trim angle	-8.41° to 11.4°	-5.84° to -2.15°
Tether tension	Max 30.4 kN	4.9 - 11.8 kN

7. TETHER PROFILE ESTIMATION

The estimation of tether profile is important as it defines the safety zone around the place of aerostat deployment. The horizontal component of tether profile is known as Blow by. The tether profile also predicts the length of tether required to maintain the aerostat envelope at a particular height. All the forces introduced by the envelope on the tether can be summed up into one force and its angle with horizontal as in Eqns. (17) and (18). It is required to estimate this force and angle for the entire tether. To achieve this, the cable is broken into rigid elements of finite length and the forces acting on this length is evaluated to obtain a magnitude and angle for lower elements. Balancing the forces on the cable elements the tension and angle for the next lower element may be written as[11]:

$$\theta_{n+1} = \tan^{-1}\left(\frac{T_n \sin\theta_n - \left(w_n + D_{w_n}\right)}{T_n \cos\theta_n + D_{H_n}}\right) \tag{19}$$

$$T_{n+1} = \frac{T_n \cos\theta_n + D_{H_n}}{\cos\theta_{n+1}} \tag{20}$$

Starting from the confluence point, we proceed downwards to estimate tether tension and angle with horizontal using Eqns. (19) and (20) till we reach winch point on the ground. The summation of horizontal component of tether length then gives blow by and summation of vertical component of tether length gives height. A typical result of tether profile estimation is presented in Fig. 11. As can be seen in Fig. 11 the 'blow by' increases with wind speed. If it is required to maintain a constant height for aerostat, as is generally the case, then additional tether length will be required to be released from the winch drum. Hence additional tether length should be catered beforehand.

8. ENVELOPE FABRICATION

Envelope should be strong, light weight and properly shaped. Resulting shape is a body of revolution with surface curvatures in all planes. Designer is faced with the challenge to pattern and construct 3-D shape out of 2-D flat fabric. But fabric being flexible material, it becomes possible. The elastic flat pieces are stretched into curves. Basic element of the envelope or ballonet is gore. Gores are made up of panels to allow proper rotation of the fabric. Hence from 3-D model of the aerostat envelope, 2-D flat patterns are developed using gore and panel combination. Finally these patterns are joined along the edges using fabric welding machine. The actual aerostat envelope in tethered and mooring condition is presented in Figs. 12 and 13.

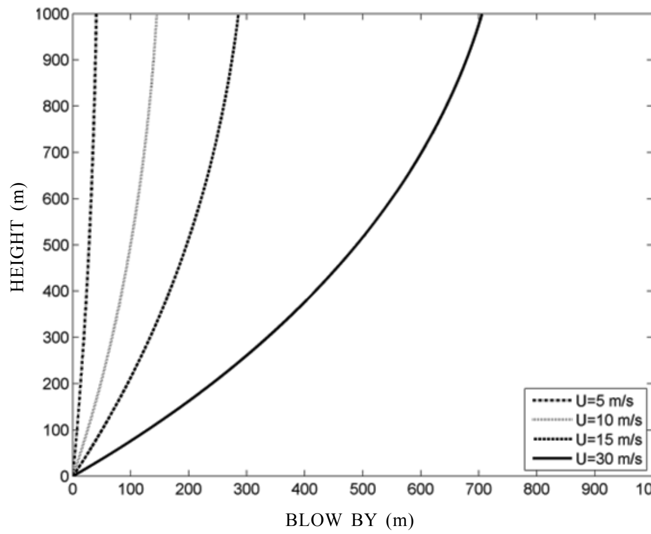

Figure 11. Tether profile for the aerostat for a typical operating condition.

Figure 12. Envelope in tethered condition.

Figure 13. Envelope in mooring condition.

9. CONCLUSIONS

The design, analysis, and realisation aspects for a medium size aerostat envelope have been presented. The line of sight coverage radius and payload requirement came out to be important parameters for selecting aerostat height and volume.

For a given payload capacity and height of operation, the volume of envelope is estimated using fundamental approach. The stress analysis has then been carried out using both analytical and finite element analysis approach. The methods for carrying out equilibrium analysis, tether tension and tether profile estimation have been presented for the given configuration. Important design parameters were estimated for the entire possible operating conditions for aerostat. A comparison of these estimated parameters and measured parameters during limited aerostat trials was also carried out. Both the estimated and measured trim angle lies within the specified range. Also the measured values of payload capacity, trim angle and tether tension during the limited flight trials of the aerostat lies within the estimated values for entire operating conditions. However, six degrees of freedom dynamic analysis of aerostat with tether will be required for better estimation of dynamic parameters.

REFERENCES

1. Colozza, A. & Dolce, J.L. High-altitude, long-endurance airships for coastal surveillance. Glenn Research Center, Report No. NASA/TM—2005-213427, pp. 5.
2. Vijayram, C. & Pant, R. Multidisciplinary shape optimization of aerostat envelopes. *J. Aircraft*, 2010, **47**(3), 1073-1076.
   doi: 10.2514/1.46744
3. Khoury, G.A. & Gillett J.D. Airship technology. Cambridge University Press, 2004.
4. Anderson John D Jr. Introduction to flight. Ed. 5th, Tata McGraw-Hill Publishing Company Limited, New Delhi, 2008.
5. Myers, Philip F. & Vorachek, Jerome J. Definition of tethered balloon systems. Goodyear Aerospace Corporation, Akron, Ohio, 1971.
6. Airship Design Criteria. US Department of transportation, federal aviation administration. No. FAA-P-8110-2, pp. 42.
7. Subramanya, H. Y.; Narendra, M.S. & Murthy, S.S. Stress analysis of 2000 m^3 aerostat for combined loading conditions. NAL, Bangalore, India, Report No. NAL – PD STTD 0806, March 2008.
8. Hunt, J.D. Structural analysis of aerostat flexible structure by finite element method. *J. Aircraft*, 1981, **19**(8), 674-678.
   doi: 10.2514/3.57448
9. Krishnamurthy, M. & Panda, G.K. Equilibrium analysis of a tethered aerostat. Project Document FE 9802, Flight Experiment Division, NAL, Bangalore, India, 1998.
10. Chapra, Steven C. Applied numerical methods with MATLAB for engineers and scientists. Ed. 3rd, McGraw-Hill Higher Education, 2011, pp. 156-168.
11. Right, John B. Computer programs for tethered-balloon system design and performance evaluation. Air Force Geophysics Laboratories, Massachusetts, Report No. AFGL-TR-76-0195, 1976.

CONTRIBUTORS

Mr A. Kumar obtained his BTech (Mechanical Engineering) from BIT Sindri in 2003 and M.Tech (Aerospace Engineering) from IISc Bangalore in 2005. Presently, he is Scientist ‘D’ in ADRDE Agra. He is mainly working in the area of : Aerostat envelope design, structural and dynamic analysis of aerostat envelope. His interests also include stress analysis and fracture mechanics.

In the current study, he has contributed in line of sight estimation, analytical stress and finite element stress analysis.

Dr S.C. Sati obtained his BTech (Mechanical Engineering) from MNR Engg College, Allahabad University, in 1979, MTech (Mechanical Engineering) from IIT Bombay, in 1996 and PhD from Pune University, in 2011. Presently, he is Director General (Naval Systems) in DRDO. He has also served as Director ADRDE Agra. His research interests include : Dynamic modelling and simulation, hydraulics, launcher design, stress analysis, aerostat and airship design.

In the current study, he has contributed in tether profile estimation.

Prof A.K. Ghosh obtained his MTech and PhD in Aerospace Engineering from IIT Kanpur. Presently he is Professor in Aerospace Engineering Department at IIT Kanpur. His research interest includes : Flight mechanics, parameter estimation from flight images, neural modelling, design of air borne stores: aircraft bombs, artillery shells and rockets design of control law of guided missiles.

In the current study, he has contributed in equilibrium analysis.